Supplement of Atmos. Chem. Phys., 17, 14239–14252, 2017
https://doi.org/10.5194/acp-17-14239-2017-supplement

Supplement of

Spatiotemporal distribution of nitrogen dioxide within and around a large-scale wind farm – a numerical case study

Jingyue Mo et al.

Correspondence to: Jianmin Ma (jianminma@lzu.edu.cn) and Tao Huang (huangt@lzu.edu.cn)

Model validation

The modeled NO_2 air concentrations from the 4 model scenarios were compared with the monitored air concentrations from 0000 UTC November 19 to 0000 UTC November 21, 2016 at the Jiuquan Air Quality Monitoring Station operated by the Jiuquan Environmental Protection Agency. Figure S1 in Supplement shows the simulated and measured NO_2 concentrations at the Jiuquan Station. The statistics between the modeled and measured data are presented in Table S1. Overall, the model results from the 4 modeling scenarios agree reasonably well with the measured data. The modeled peak concentrations from S2 lagged 2 hours behind the observed value, and the modeling results from S1, S3 and S4 lagged 4 hours behind the measured data, respectively.

As an operational weather forecasting model, the WRF model has been evaluated extensively. In the present study, we further compared WRF simulated winds and temperatures from the 4 modeling scenarios with measured data near the surface. There are three routine weather stations within the fine model domain. They are Mazongshan (52323), Dunhuang (52418), and Jiuquan (52533) stations. Measured and WRF simulated hourly winds and temperatures at these three stations from 0000 UTC November 19 to 0000 UTC November 21 2016 are displayed in Figure S2. As shown, the WRF simulated wind speeds and temperatures from the 4 model scenarios captured the magnitude and the diurnal variation of the observed data at these three weather stations (Fig. S2a–f), except for Figures S3 and S4 are the correlation diagrams between the measured and modeled temperatures (Fig. S3) and wind speeds (Fig. S4) at these 3 stations, respectively. The simulated temperatures agree well with the measurements at the three stations with the coefficient of determination $R^2 = 0.93$ for the model scenarios S1, S3, and S4, and 0.84 for S2. The relatively lower R^2 value was likely due to a large deviation of the modeled temperature from observed value at Mazongshan station in the second day (November 20 2016). As shown in Fig. S2 (a), WRF model in S2 scenario did not predict the peak value of air temperatures on the second day (November 20 2016) as shown in the measured data (Fig. S2a).

Table S1. Statistics between modeled and measured hourly NO_2 air concentrations

	R (correlation coefficient)	AE (absolute error)	FE (fractional error)	FB (fractional bias)
S1	0.74360 (p=1.41E-9)	0.00488	0.61642	0.00996
S2	0.72185 (p=7.05E-9)	0.00470	0.62850	0.00055
S3	0.71755 (p=9.52E-9)	0.00491	0.62369	0.00108
S4	0.71875 (p=8.76E-9)	0.00490	0.62188	0.00100

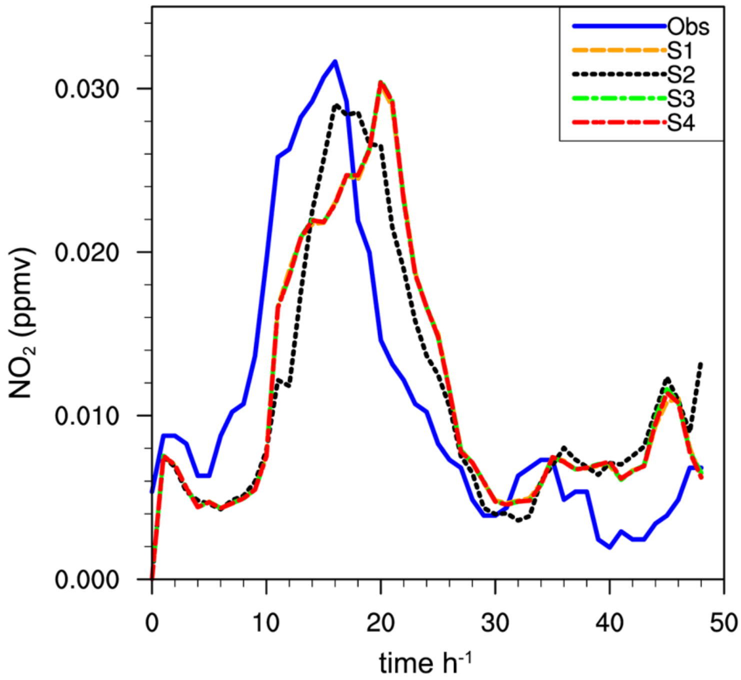

Figure S1. Modeled and measured hourly concentrations of NO_2 at Jiuquan from 0000 UTC November 19 to 0000 UTC November 21 2016. Blue solid line denotes measured data, black dashed lines stand for simulated concentrations from S2, and brown, green and red dashed lines denote simulated concentrations from S1, S3 and S4 which are overlapped in the figure.

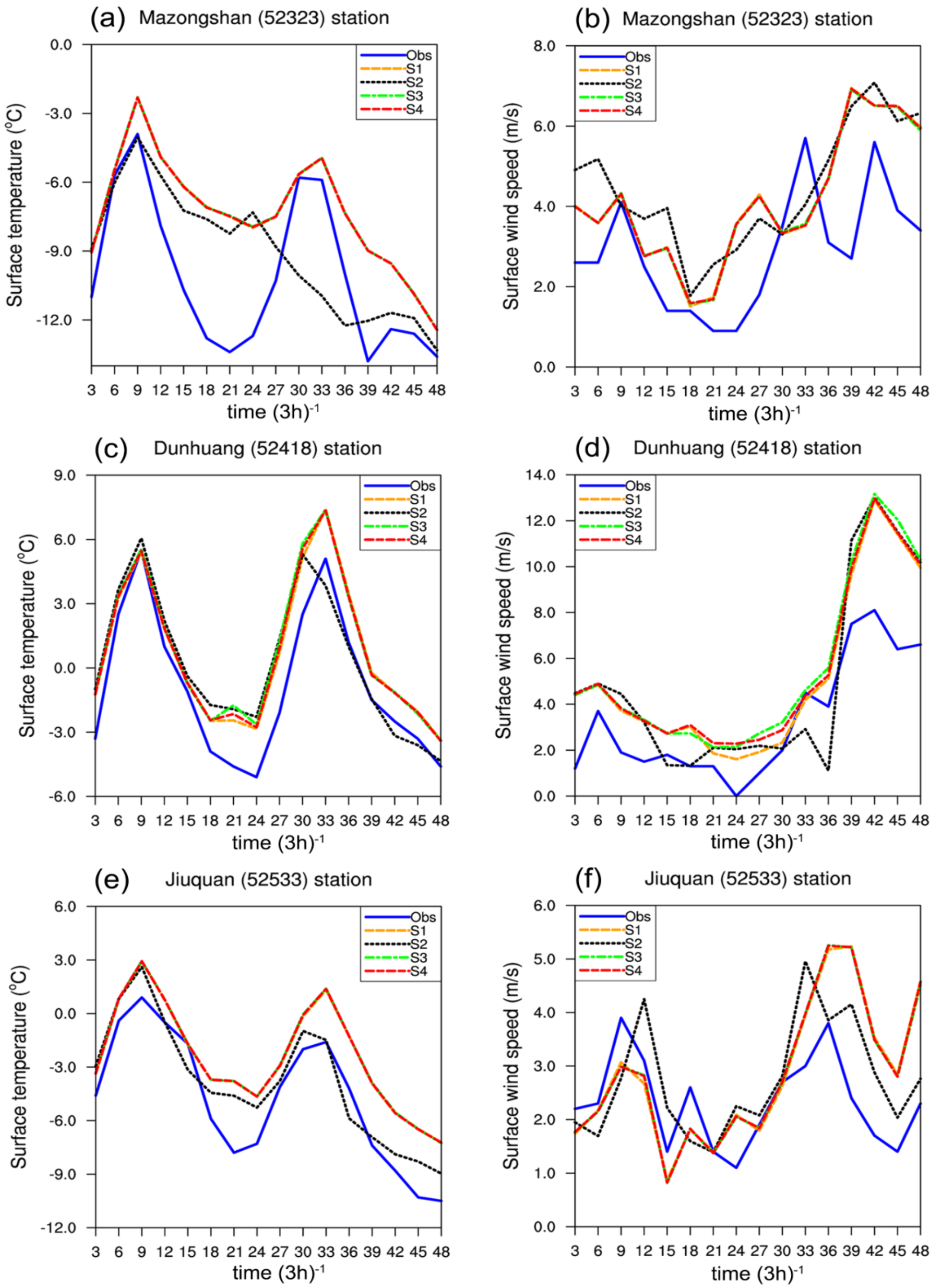

Figure S2. Modeled and measured hourly temperature (°C) and wind speed (m s^{-1}) for every 3 hours from 0000 UTC November 19 to 0000 UTC November 21 2016 at Mazongshan (52323), Dunhuang (52418) and Jiuquan (52533) meteorological stations. Temperatures at these three sites are illustrated on the left panel (Fig. S2(a), (c), and (e)); and wind speeds are displayed on the right panel (Fig. S2(b), (d), and (f)).

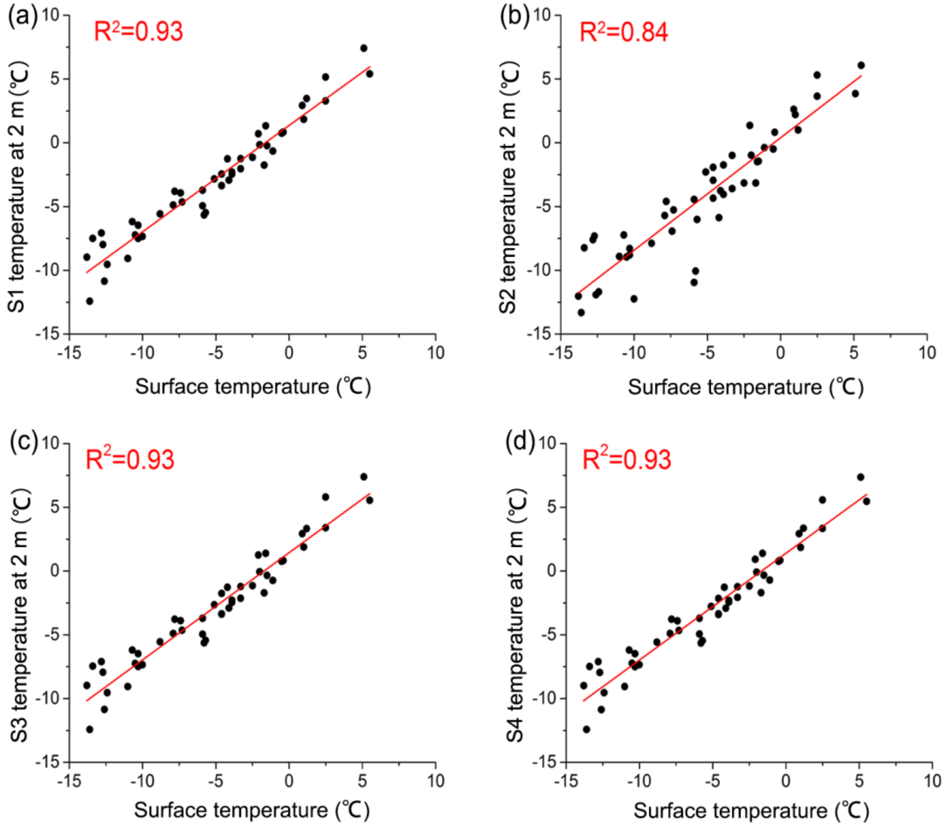

Figure S3. Correlation diagrams for measured and modeled surface air temperatures (^{o}C) at the 1.5 m height at Mazongshan (52323), Dunhuang (52418) and Jiuquan (52533) weather stations in (a) model scenario S1 (b) model scenario S2, (c) model scenario S3, and (d) model scenario S4.

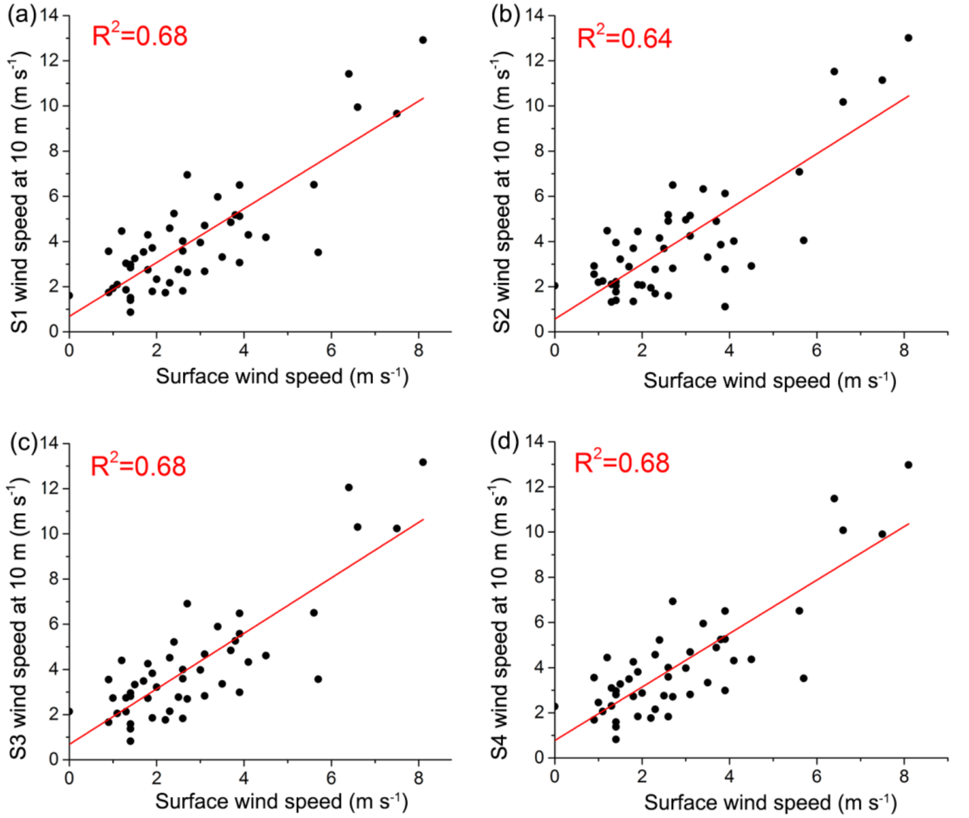

Figure S4. Correlation diagrams for measured and modeled surface wind speeds (m s^{-1}) at the 10 m height at Mazongshan (52323), Dunhuang (52418) and Jiuquan (52533) meteorological observation at (a) model scenario S1 (b) model scenario S2, (c) model scenario S3, and (d) model scenario S4.

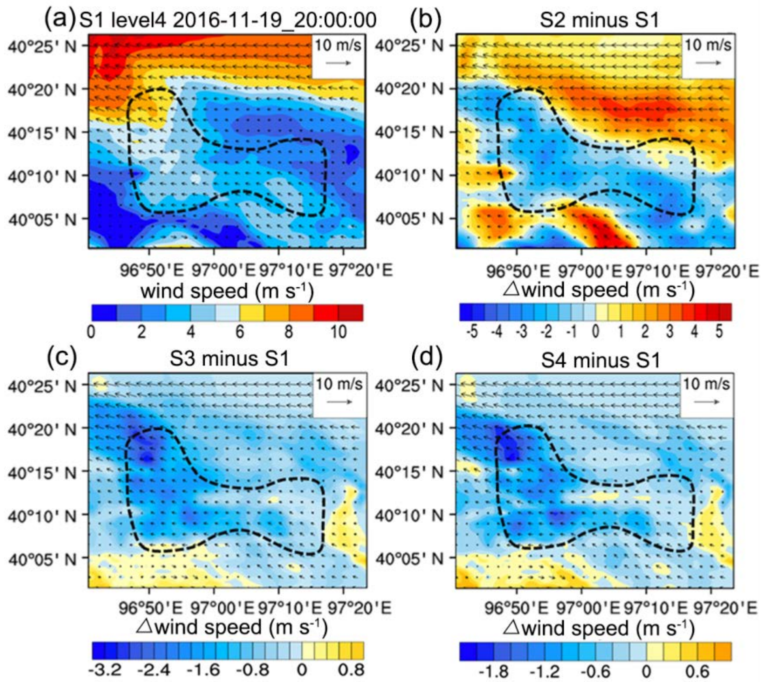

Figure S5. Wind field predicted by the control run (a) and the differences (ΔV) between the wind fields by three wind farm parameterizations and the wind field from the control run at 2000 UTC November 19 at the 4th model level (~100 m). (b) $\Delta V = V_{S2} - V_{S1}$, (c) $\Delta V = V_{S3} - V_{S1}$, (d) $\Delta V = V_{S4} - V_{S1}$, where V_{S1}, V_{S2}, V_{S3}, and V_{S4} are winds predicted by model scenarios 1–4.

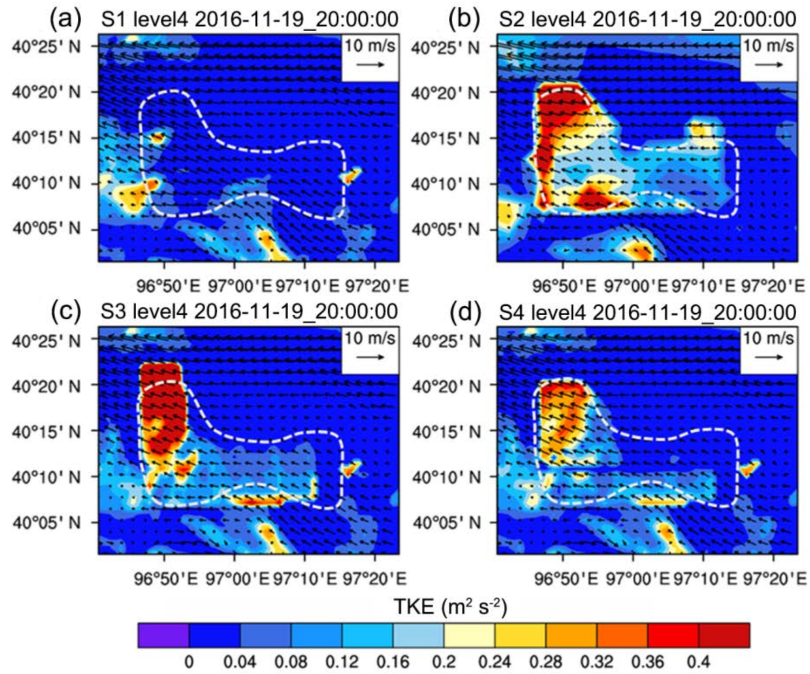

Figure S6. Modeled TKE contour and vector winds by four model scenario run at 2000 UTC on November 19th, 2016 (m^2 s^{-2}), within the YWF (marked by white dashed line) and its surrounding that indicated by the white box in Figure 2 at the eta level 4 about 100m the reference vector is 10 m s^{-1}. (a) TKE by the control scenario run (S1), (b) TKE by model scenario 2 (roughness length parameterization), (c) TKE by model scenario 3 (drag force parameterization with high density wind turbines setup), (d) TKE by model scenario 4 (wind turbine drag force parameterization with low density wind turbines setup).